Catalysis Today xxx (2016) xxx–xxx

Contents lists available at ScienceDirect

Catalysis Today

journal homepage: www.elsevier.com/locate/cattod

Anodization of bismuth doped TiO_2 nanotubes composite for photocatalytic degradation of phenol in visible light

Imran Ali, Seu-Run Kim, Sung-Pil Kim, Jong-Oh Kim*

Department of Civil and Environmental Engineering, Hanyang University, 222 Wangsimni-ro, Seongdong-gu, Seoul 133-791, Republic of Korea

ARTICLE INFO

Article history:
Received 27 November 2015
Received in revised form 7 March 2016
Accepted 22 March 2016
Available online xxx

Keywords:
Anodization
Bismuth doping
TiO_2 nanotubes
Organic pollutant
Phenol
Photocatalytic degradation

ABSTRACT

Bismuth doped TiO_2 photocatalyst was synthesized in a one-step electrochemical anodization method. Bismuth nitrate $Bi(NO_3)_3$ was used as a bismuth source. The obtained samples were characterized by FE-SEM, XRD, EDX and XPS. The optimum synthesis conditions for bismuth doping were 1.0 M bismuth nitrate in an ethylene glycol electrolyte with anodization at 40 V for 2 h. Compared with undoped TiO_2 nanotubes, bismuth doped TiO_2 photocatalyst showed a higher photocatalytic activity by a factor of 4.0 for phenol degradation under visible light irradiation. The optimum phenol degradation using a photo-electrocatalytic method was observed at a 0.5 V external bias, and this degradation rate was 5.2 times faster than that observed for undoped TiO_2 nanotubes. The doped bismuth TiO_2 nanotubes are favorable for the separation of photo-induced electrons and holes, reducing the recombination of charges, and promoting the formation of hydroxyl radicals and superoxides that degrade phenol.

1. Introduction

Phenol is commonly used in many industries as a precursor, and it is also a representative contaminant in industrial wastewater effluents [1]. Phenol has negative effects on marine life and aquatic environments when it is discharged in-to streams [2]. Phenol from wastewater can be removed by conventional technologies like adsorption, coagulation, and enzyme oxidation [3–5]. However, these conventional technologies do not completely degrade the organic pollutants and can produce secondary pollutants [6].

In recent years, great progress has been made in the photocatalytic degradation of organic pollutants using semiconductor-based nanomaterials [7]. TiO_2-based nanomaterials have been intensively studied and widely used [8] because of their high photocatalytic activity, low cost, recyclability and ability to oxidize and reduce most organic pollutants [9]. TiO_2 generates hydroxyl (OH) radicals, which are more powerful than ozone and other advanced oxidation processes (AOPs) used to degrade organic pollutants. However, TiO_2 has low photocatalytic efficiency in visible light because its band gap energy (3.0–3.2 eV) must be activated by ultraviolet (UV) light, and solar light contains only 5% UV light [10]. Furthermore, TiO_2 shows high recombination rate between electron (e^-) and hole (h^+) pairs. To overcome these problems, different strategies have been used to modify the TiO_2 surface including metal deposition (e.g., Pt and Fe [11–13]) non-metal doping with N and S [14,15], and coupling with other semiconductors CdS, WO_3 and MnO_2 [16,17].

Research in visible light response photocatalysts has recently become popular and has focused on materials like $BiVO_4$, BiOI, and $BaIn_2O_4$ [2,18,19]. Bismuth nanomaterials are used as a photocatalyst due to their unique layered and suitable band structure, non-toxic nature, high chemical stability [2,20] and band gap energy of 1.8–2.4 eV, which is in the visible light region [21]. Bismuth oxide (Bi_2O_3) is a new type of visible light responsive photocatalyst that has a wide range of applications. Composites of bismuth and TiO_2 nanomaterials show good photocatalytic results as compared to using each alone [22,23]. Bismuth oxide is a p-type semiconductor having conduction and valance band edges of +0.336 and +0.130 (vs. NHE), respectively [24]. Bismuth on the surface of TiO_2 can trap photo-generated e^-, thus reducing recombination of e- and h^+ pairs, and enhance the photocatalytic activity of TiO_2 under visible light irradiation [25].

Anodization is a useful technique for modifying the surface of a Ti substrate to obtain a nanotubular structure [26]. Many researchers have used Bi_2O_3 as a doping material to modify the surface of anodized TiO_2 nanotubes (TNT) with different bismuth doping strategies like hydrothermal deposition [27], dip-coating methods [28], and electrochemical deposition [29]. These TNT modifications were performed in a two-step process beginning with anodization of TNT followed by bismuth doping. To solve this

* Corresponding author.
E-mail addresses: jk120@hanyang.ac.kr, jongohkim1221@gmail.com (J.-O. Kim).

http://dx.doi.org/10.1016/j.cattod.2016.03.029
0920-5861/

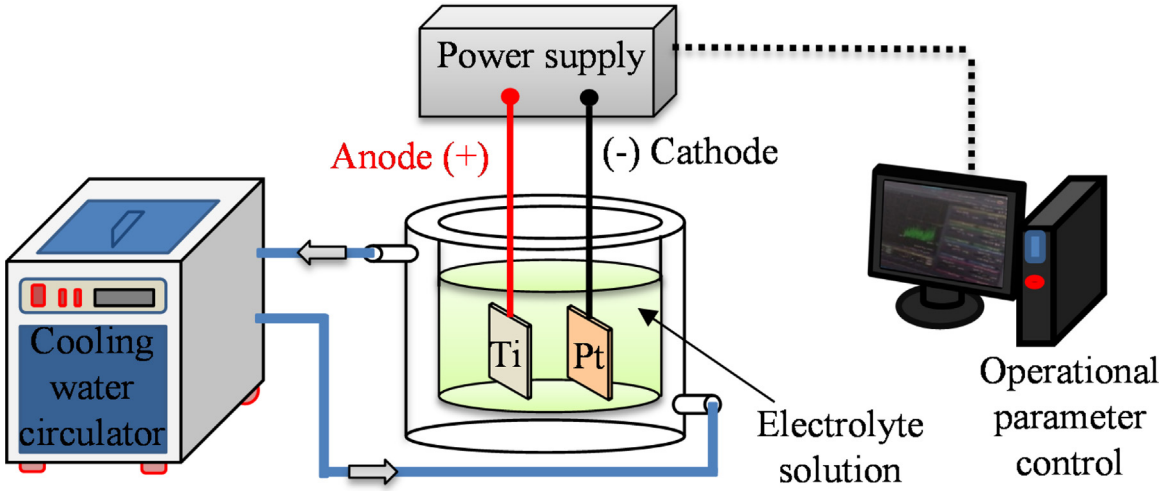

Fig. 1. Anodization equipment setup with power supply and operational parameter control.

two-step experimental process, in our study we proposed one-step synthesis method. This reported synthesis method has high technical accessibility, low energy consumption, and less time required for synthesis.

In this study, we fabricated bismuth doped TiO_2 nanotube (Bi-TNT) composites with a new one-step electrochemical anodization method. To our knowledge, no one has worked on this type of bismuth modification before. Bismuth was doped on TNT using different bismuth nitrate concentrations, anodization voltages and times. Then, Bi-TNT catalyst was used for photocatalytic (PC) and photoelectrocatalytic (PEC) degradation of phenol under visible light irradiation. Also, PEC degradation of phenol was monitored at different external biases (0.1–1.0 V).

2. Experimental

2.1. Materials and chemicals

Ti foil (purity of 99.5%, $2 \times 5\,cm^2$ in size with a thickness of 0.25 mm) was purchased from Alfa Aesar, Korea. Ethylene glycol (94.5%) and bismuth nitrate (98.0%) were purchased from Daejung Chemicals & Metal Co. Ltd., Korea. NH_4F (97.0%) was purchased from Junsei Chemical Co. Ltd., Japan. All chemicals were of analytical grade and were used as received.

2.2. One-step synthesis of Bi-TNT

Ti foil was sonicated in acetone, ethanol and deionized (DI) water for 10 min each to remove impurities. The foils were then dried in N_2 gas. We used an electrolyte solution of ethylene glycol with 3 wt% NH_4F, 5 wt% DI water and different bismuth nitrate concentrations (0.5–1.5 M) as shown in Table 1. Ti foil was used as an anode and platinum (Pt) as a cathode. The distance between two electrodes was kept at 2 cm. Anodization was performed at different voltages (30–50 V) and times (1–3 h) using a power supply (N6702A Agilent Technologies, Spain) as shown in Fig. 1. After anodization, the Ti foil was rinsed in DI water and dried in N_2 gas. Annealing was performed at 550 °C for 1.5 h in a furnace to improve the anatase crystalline structure of the TiO_2.

2.3. Characterization

The surface morphology of the synthesized catalyst was examined using field emission scanning electron microscopy (FE-SEM, Sigma, Carl Zeiss Co., Germany). The crystal structure was analyzed using X-ray diffraction (XRD, D8-Advance, Bruker-AXS Co., Germany). Elemental analysis and the chemical composition of the catalyst was examined using energy dispersive X-ray spectroscopy (EDX, Noran System 7, Thermo Scientific, USA) and X-ray photoelectron spectroscopy (XPS, Thermo Fisher Scientific Co., USA).

Table 1
Bismuth doping on TNT with different electrolyte concentrations and anodization parameters.

Order	Electrolyte (M)	Anodization	
	Bismuth nitrate	Time (h)	Voltage (V)
1	0.5	1	30
2	0.5	2	30
3	0.5	3	30
4	0.5	2	40
5	0.5	2	50
6	1.0	2	30
7	1.0	2	40
8	1.0	2	50
9	1.5	2	30

M = mole.

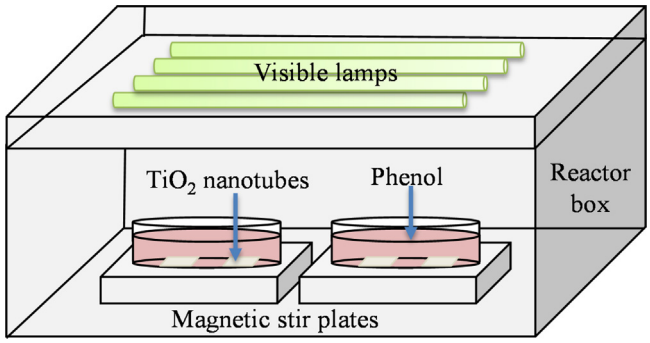

Fig. 2. Schematic diagram of photocatalytic reactor prepared in the lab.

2.4. Photocatalytic test

The photocatalytic performance of the synthesized sample was investigated towards photodegradation of phenol. The initial phenol concentration was 50 mg L^{-1} and a 40 mL solution was used in a reactor (prepared at lab scale) as shown in Fig. 2. The total catalyst (Ti foil) area used for the photocatalytic test was 32 cm^2.

Please cite this article in press as: I. Ali, et al., Anodization of bismuth doped TiO_2 nanotubes composite for photocatalytic degradation of phenol in visible light, Catal. Today (2016), http://dx.doi.org/10.1016/j.cattod.2016.03.029

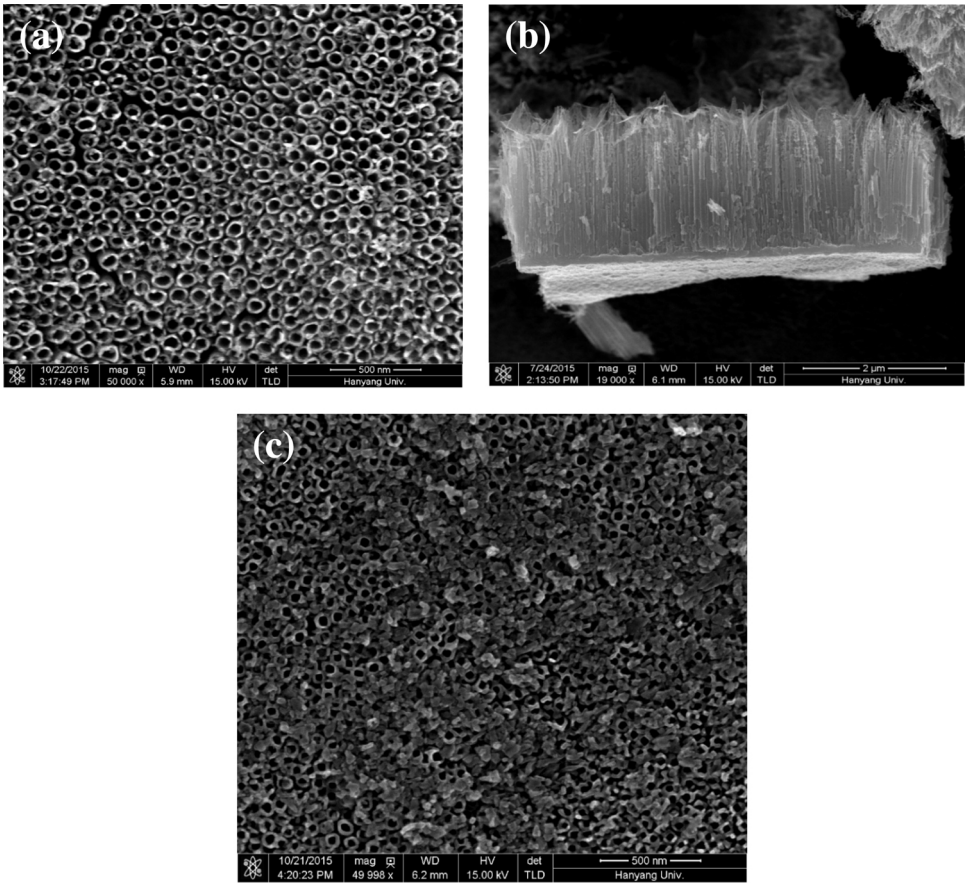

Fig. 3. FE-SEM images of (a) TNT, (b) side view of TNT, and (c) Bi-TNT.

The PC activity test was performed under a visible light source (Fluorescent lamp 32 W, λ = 400–700 nm, Philips Co., Netherland), and the UV cut-off filter λ < 420 nm at room temperature. PEC activity was performed at different voltages (0.1–1.0 V). Initially, the samples were kept in the dark for 1 h to achieve adsorption equilibrium. Later, visible light irradiation was supplied to perform PC and PEC experiments. The amount of phenol degradation was determined using a UV–vis spectrophotometer (UV mini 1240, Shimadzu, USA) using the peak at a wavelength of 270 nm [15,30]. The intermediate products of phenol were analysed using gas chromatography (GC, Shimadzu, GC-2010, Japan) and mass spectrometry (MS, Shimadzu GCMS-QP2010, Japan) with a thermal desorber (TD, UNITY II, Markes International, Ltd., UK) system. The details of the TD-GC-MS method is given in Supplementary materials and Table 1S.

3. Results and discussion

3.1. Characterization

3.1.1. FE-SEM

Typical FE-SEM images of TNT and Bi-TNT samples are shown in Fig. 3. It is clear that TiO_2 nanotubes were successfully fabricated on Ti foil by anodization, and the average nanotube diameters were approximately 50 nm, and length was 2000 nm as shown in Fig. 3(a) and (b), respectively. Most of the nanotubes were uniform in size and highly oriented. TiO_2 nanotubes were well-separated from each other and tube mouths were open. The optimum synthesis conditions for bismuth doping were found at a bismuth nitrate concentrations of 1.0 M with anodization at 40 V for 2 h as shown in Fig. 3(c). The FE-SEM images of other synthesis conditions are shown in Supplementary materials Fig. 1S. The FE-SEM clearly shows that a thin layer of bismuth oxide formed on the TNT surface, and tube-like structures were still present after bismuth doping.

Table 2
The element analysis of EDX spectrum of Bi-TNT composite.

Element	Ti	O	C	Bi
At%	20.3	71.6	6.7	1.4
Wt%	41.3	48.8	3.4	6.5

3.1.2. XRD

The XRD patterns showed that the undoped TNT and Bi-TNT samples exhibited a crystalline anatase phase after being annealed at 550 °C as shown in Fig. 4(a) and (b), respectively. Bismuth peaks were observed with Ti peaks, and Ti was converted to an anatase crystalline phase while Bi was converted to bismuth oxide. The Bi species were present in a separate phase of bismuth oxide. The peaks at 27.4, 47.1 and 56.0 two theta were identified as the main peaks of bismuth oxide [23,25,29].

3.1.3. EDX and XPS

The quantitative analysis of the Bi-TNT composite was obtained by EDX spectrum. As shown in Fig. 5(a) the deposit mainly consisted of Bi [31,32]. The carbon peak observed in the EDX spectrum may have been due to contamination. The atomic concentrations of Ti, Bi and O were 20.3, 1.4 and 71.6 at%, respectively as shown in Table 2.

The wide scan XPS spectrum of the Bi-TNT composite is shown in Fig. 5(b). Ti 2p and O 1s peaks were observed at binding energies of about 469 and 530 eV, respectively. The Bi 4f peaks were observed

Please cite this article in press as: I. Ali, et al., Anodization of bismuth doped TiO_2 nanotubes composite for photocatalytic degradation of phenol in visible light, Catal. Today (2016), http://dx.doi.org/10.1016/j.cattod.2016.03.029

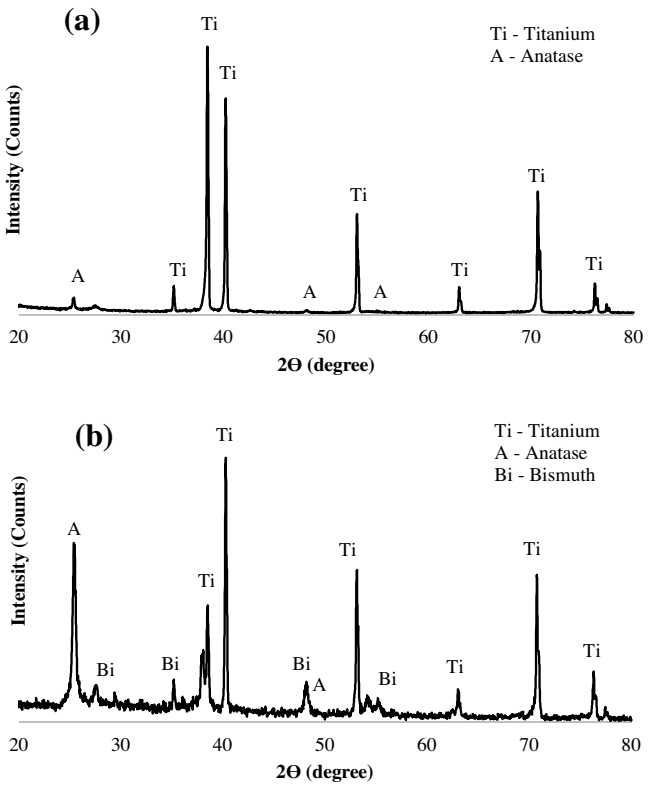

Fig. 4. XRD patterns of (a) TNT and (b) Bi-TNT samples.

at 158 and 163 eV [28,29,33]. Based on these results we confirmed that bismuth was successfully doped onto the TNT surface.

3.2. Photocatalytic degradation of phenol

3.2.1. PC and PEC activity

Photodegradation of phenol was conducted to evaluate the photocatalytic activity of Bi doped TiO_2 catalyst. Fig. 6(a) and (b) shows the degradation rate of phenol relative to undoped TNT and Bi-TNT samples under visible light irradiation for 8 h. No phenol degradation was observed when the experiment was performed under photolysis or catalysis. This control experiment confirmed that TiO_2 requires light source for activation to remove organic pollutant [22]. The phenol photocatalytic degradation rate of the Bi-TNT sample was higher than that of undoped TNT. The phenol degradation was 4.4, 7.7, 17.5, and 40.3% by TNT PC, TNT PEC, Bi-TNT PC, and Bi-TNT PEC, respectively [34]. The Bi-TNT sample (optimum synthesis condition of bismuth nitrate 1.0 M, anodization at 40 V for 2 h) showed a higher phenol degradation rate by a factor of 4.0 as compared with undoped TNT when operating in PC mode. In terms of PEC activity, phenol degradation was higher than undoped TNT by a factor of 5.2 at a 0.5 V external bias.

To check the effect of external bias on the degradation of phenol, PEC activity was performed at different external biases (0.1 ~ 1.0 V) as shown in Fig. 7(a) and (b). The phenol degradation was 25.3, 34.4, 40.3, 35.7, and 31.2% at an external voltage of 0.1, 0.3, 0.5, 0.7, and 1.0 v respectively. The optimum phenol degradation was found at 0.5 V under visible light irradiation. The PEC activity of phenol degradation increased with increasing applied voltage upto 0.5 V, but then decrease thereafter. The decrease in phenol degradation above 0.5 V was because excess voltage caused a recombination

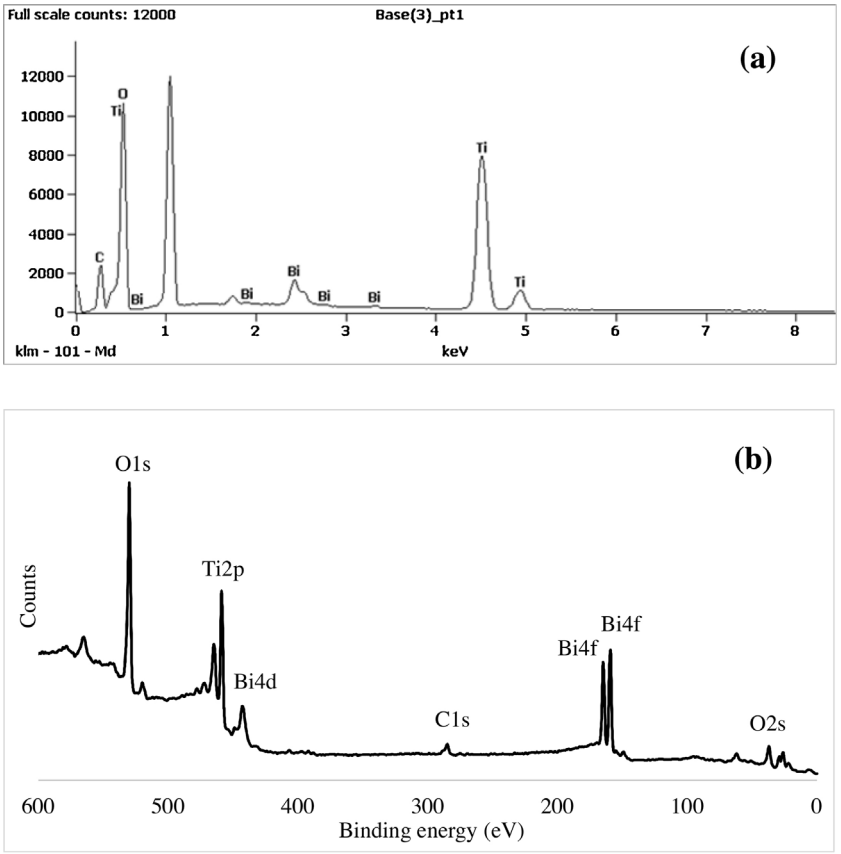

Fig. 5. Bi-TNT sample data: (a) EDX spectrum and (b) XPS spectrum.

Please cite this article in press as: I. Ali, et al., Anodization of bismuth doped TiO_2 nanotubes composite for photocatalytic degradation of phenol in visible light, Catal. Today (2016), http://dx.doi.org/10.1016/j.cattod.2016.03.029

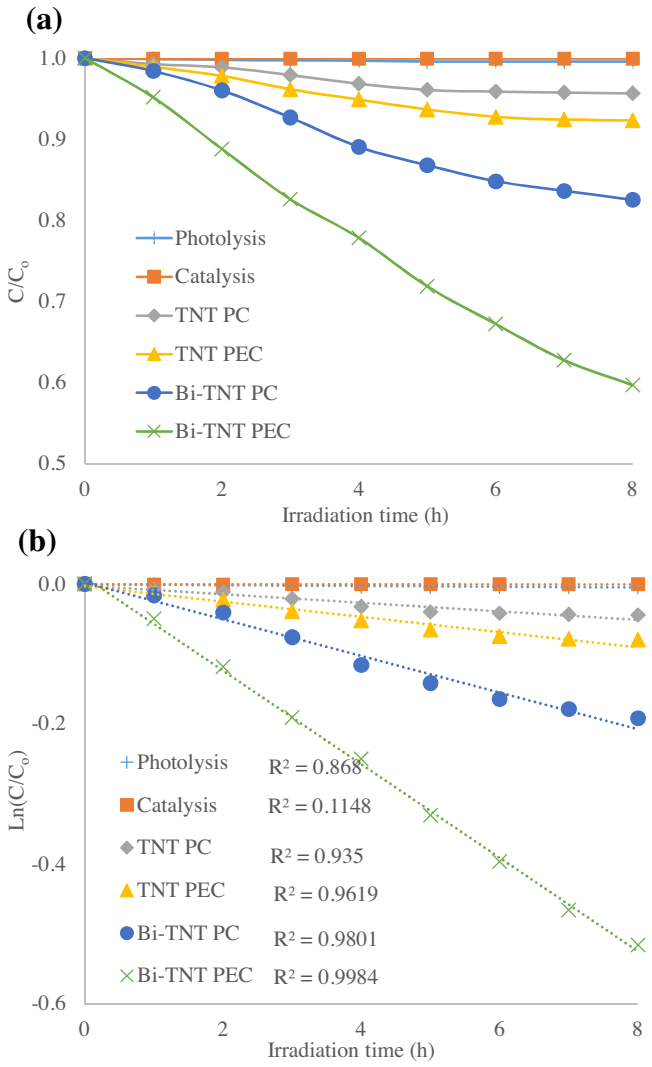

Fig. 6. Degradation of phenol under visible light: comparison of PC and PEC process (a) C/C_o and (b) $Ln(C/C_o)$.

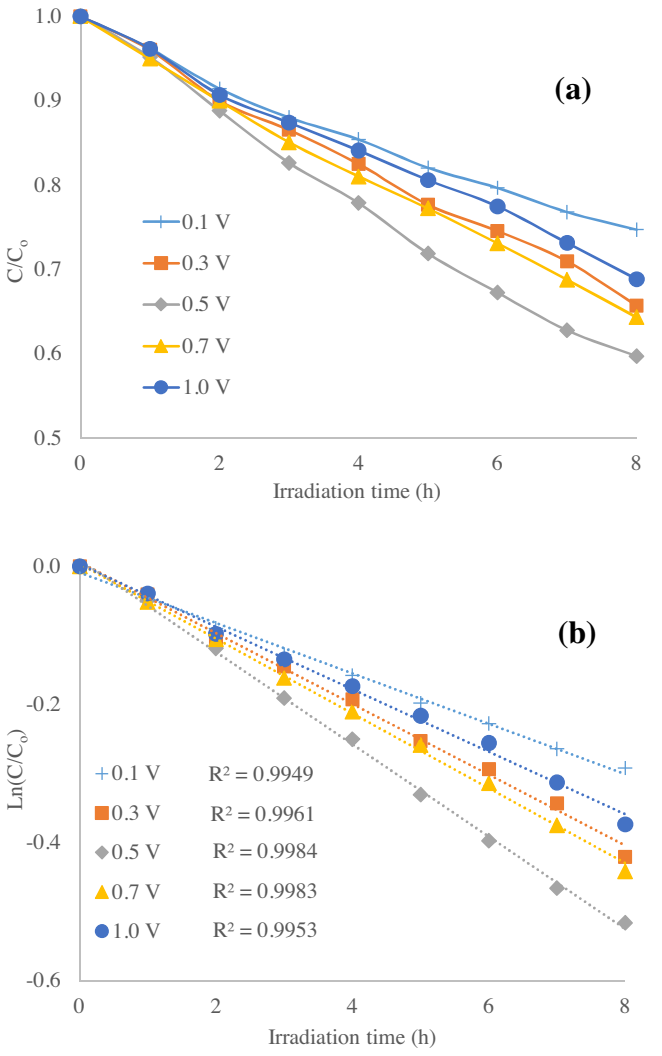

Fig. 7. Effect of external volt on PEC process for phenol degradation under visible light (a) C/C_o and (b) $Ln(C/C_o)$.

Table 3
The reaction rate constant k, and the associated R^2 values of different phenol degradation processes.

Process	V	Rate constant k 10^{-2} h^{-1}	R^2
Photolysis		0.05	0.8680
Catalysis		0.01	0.1148
TNT PC		0.56	0.9350
TNT PEC	0.5	1.00	0.9619
Bi-TNT PC		2.40	0.9801
Bi-TNT PEC	0.1	3.65	0.9949
Bi-TNT PEC	0.3	5.26	0.9961
Bi-TNT PEC	0.5	6.45	0.9984
Bi-TNT PEC	0.7	5.52	0.9983
Bi-TNT PEC	1.0	4.67	0.9953

reaction between electrons from the additional applied voltage and holes formed on TiO_2 [35].

The reaction rate constant was calculated according to Eq. (1) [36],

$$Ln(C/C_o) = -kt \quad (1)$$

here C is the concentration at particular time, C_o is the initial concentration, k is a first order rate constant (h^{-1}), and t is reaction time in h. Table 3 shows a summary of the reaction rate constant k and its associated R^2 values. The PEC activity of Bi-TNT sample at 0.5 V had a higher reaction rate constant than other samples, and this sample showed higher phenol degradation activity.

The higher photocatalytic activity of Bi doping observed here may be due to the following reasons. First, Bi doping can reduce the band gap energy, which significantly improves the absorption of TiO_2 in visible light [37]. Secondly, Bi doped on the surface of TiO_2 can trap photogenerated electrons thereby suppressing the recombination of electrons and holes [38]. This promotes the formation of OH radicals and superoxides. Meanwhile, the specific surface areas of composite samples are large [39], which favour the adsorption of organic compounds and provide more accessible active sites.

3.2.2. Phenol degradation mechanism

Here we proposed a possible mechanism for the effects of bismuth, which is illustrated in Fig. 8. This mechanism includes following steps: (i) visible light irradiation on TiO_2 surface enhanced by the bismuth doping, (ii) the excitation of photoinduced electrons from the valence band (VB) to the conduction band (CB) of TiO_2, resulted the generation of holes in the VB of the bismuth (iii) the created e^- and h^+ initially reacts with H_2O, and (iv) induced the degradation of organic pollutant [40]. Bismuth enhanced the photocatalytic activity of TiO_2 under visible light irradiation. Consequently, more photons from visible irradiation are utilized to generate electrons and holes. Moreover, bismuth in the modified

Please cite this article in press as: I. Ali, et al., Anodization of bismuth doped TiO_2 nanotubes composite for photocatalytic degradation of phenol in visible light, Catal. Today (2016), http://dx.doi.org/10.1016/j.cattod.2016.03.029

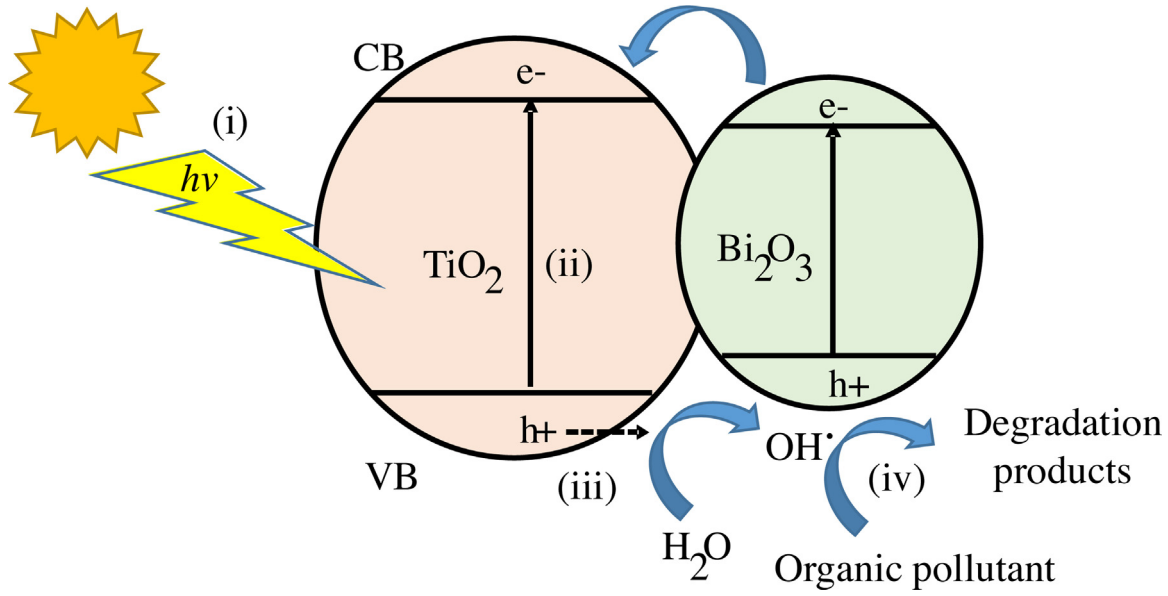

Fig. 8. Mechanism of bismuth doped TiO_2 photocatalysis.

TiO_2 systems improve the separation efficiency of photogenerated electrons and holes and produce more OH radicals and superoxides, which play an important role in the photocatalytic degradation of phenol [34].

Possible reactions related to organic pollutants degradation are shown in Eqs. (2)–(8). Bismuth doped TiO_2 photocatalyst under visible light irradiation generates e^- and h^+. The generated h^+ on the Bi surface interacts with H_2O or hydroxide ions (OH^-) produces OH radicals, and the interaction of e^- with O_2 generates superoxides ($O_2^{\bullet -}$). These OH radicals, superoxides and h^+ degraded organic pollutants into oxidized products [41].

$$\text{Bismuth}/TiO_2 + hv \rightarrow TiO_2(e^-) + \text{Bismuth}(h^+) \quad (2)$$

$$H_2O + h^+ \rightarrow OH. + H^+ \quad (3)$$

$$OH^- + h^+ \rightarrow OH^{\bullet} \quad (4)$$

$$e^- + O2 \rightarrow O_2^{\bullet -} \quad (5)$$

$$\text{Organicpollutant} + OH^{\bullet} \rightarrow \text{degradedproducts} \quad (6)$$

$$\text{Organicpollutant} + O_2^{\bullet -} \rightarrow \text{degradedproducts} \quad (7)$$

$$\text{Organicpollutant} + h^+ \rightarrow \text{degradedproducts} \quad (8)$$

Based on the TD-GC-MS analysis, the intermediate products after phenol degradation were identified as glycerol, benzene,1,1′-methylenebis[4-isocyanato-, propylene glycol, tetrahydrofuran, and acetone. The details of these intermediate products are shown in Supplementary materials Table 2S. One of the identified intermediate product glycerol was observed in previous studies by Azevedo et al. [42,43]; however, none of the intermediate products were similar to those found by Jin et al. [44].

4. Conclusions

Doping of bismuth on TiO_2 nanotubes was successfully performed and confirmed by FE-SEM, XRD, EDX and XPS. A Bi-TNT composite was made by a one-step electrochemical anodization method. The optimum synthesis conditions for bismuth doping were 1.0 M bismuth nitrate with anodization at 40 V for 2 h. This sample showed a high photocatalytic activity for phenol degradation under visible light irradiation. Photocatalytic activity of a doped sample was higher by a factor of 4.0 than an undoped TNT sample. Photoelectrocatalytic activity was higher by a factor of 5.2 at a 0.5 V external bias. The bismuth doped TiO_2 photocatalyst showed efficient separation of photogenerated electrons and holes. The phenol removal is due to the formation of OH radicals, holes, and superoxides. We observed an increased photocatalytic activity of Bi-TNT in visible light due to the bismuth doping.

Acknowledgments

This study was supported by a National Research Foundation of Korea (NRF) grant funded by the Korean Government (NRF-2016R1A2A1A05005388).

Appendix A. Supplementary data

Supplementary data associated with this article can be found, in the online version, at http://dx.doi.org/10.1016/j.cattod.2016.03.029.

References

[1] Q. Zheng, H.-J. Lee, J. Lee, W. Choi, N.-B. Park, C. Lee, Chem. Eng. J. 249 (2014) 285–292.
[2] M. Niu, R. Zhu, F. Tian, K. Song, G. Cao, F. Ouyang, Catal. Today 258 (2015) 585–594.
[3] F. Shahrezaei, Y. Mansouri, A.A.L. Zinatizadeh, A. Akhbari, Powder Technol. 221 (2012) 203–212.
[4] N. Kashif, F. Ouyang, J. Environ. Sci. 21 (2009) 527–533.
[5] J. Gómez, A. Bódalo, E. Gómez, A. Hidalgo, M. Gómez, M. Murcia, Chem. Eng. J. 145 (2008) 142–148.
[6] H. Ling, K. Kim, Z. Liu, J. Shi, X. Zhu, J. Huang, Catal. Today 258 (2015) 96–102.
[7] W.-Y. Choi, Y.-W. Lee, J.-O. Kim, Desalin. Water Treat. 34 (2011) 229–233.
[8] Q. Li, L. Zong, C. Li, J. Yang, Appl. Surf. Sci. 314 (2014) 458–463.
[9] S. Anandan, Y. Ikuma, K. Niwa, Solid State Phenom. 162 (2010) 239–260.
[10] A. Zielińska-Jurek, J. Hupka, Catal. Today 230 (2014) 181–187.
[11] M. Kitano, M. Takeuchi, M. Matsuoka, J.M. Thomas, M. Anpo, Catal. Today 120 (2007) 133–138.
[12] C. Adán, J. Carbajo, A. Bahamonde, A. Martínez-Arias, Catal. Today 143 (2009) 247–252.
[13] S.-P. Kim, J.-O. Kim, Desalin. Water Treat. (2015) 1–7.
[14] J. Yu, M. Zhou, B. Cheng, X. Zhao, J. Catal. Mol. A Chem. 246 (2006) 176–184.
[15] Y. Niu, M. Xing, J. Zhang, B. Tian, Catal. Today 201 (2013) 159–166.
[16] D. Robert, Catal. Today 122 (2007) 20–26.
[17] S. Li, Z. Ma, J. Zhang, Y. Wu, Y. Gong, Catal. Today 139 (2008) 109–112.
[18] D. Shu, J. Wu, Y. Gong, S. Li, L. Hu, Y. Yang, C. He, Catal. Today 224 (2014) 13–20.
[19] J. Tang, Z. Zou, M. Katagiri, T. Kako, J. Ye, Catal. Today 93 (2004) 885–889.
[20] J. Li, Y. Yu, L. Zhang, Nanoscale 6 (2014) 8473–8488.

[21] X. Zhang, Z. Ai, F. Jia, L. Zhang, J. Phys. Chem. C 112 (2008) 747–753.
[22] F. Duo, Y. Wang, C. Fan, X. Mao, X. Zhang, Y. Wang, J. Liu, Mater. Charact. 99 (2015) 8–16.
[23] X. Zhao, H. Liu, J. Qu, Appl. Surf. Sci. 257 (2011) 4621–4624.
[24] S.Y. Chai, Y.J. Kim, M.H. Jung, A.K. Chakraborty, D. Jung, W.I. Lee, J. Catal. 262 (2009) 144–149.
[25] D. Li, Y. Zhang, Y. Zhang, X. Zhou, S. Guo, J. Hazard. Mater. 258 (2013) 42–49.
[26] W.-Y. Choi, J. Chung, C.-H. Cho, J.-O. Kim, Desalination 279 (2011) 359–366.
[27] K. Raja, Y. Smith, N. Kondamudi, A. Manivannan, M. Misra, V.R. Subramanian, Electrochem. Solid-State Lett. 14 (2011) F5–F8.
[28] Y. Zhang, J. Lu, M.R. Hoffmann, Q. Wang, Y. Cong, Q. Wang, H. Jin, RSC Adv. 5 (2015) 48983–48991.
[29] B. Sarma, A.L. Jurovitzki, Y.R. Smith, S.K. Mohanty, M. Misra, ACS Appl. Mater. Interfaces 5 (2013) 1688–1697.
[30] H. Ling, K. Kim, Z. Liu, J. Shi, X. Zhu, J. Huang, Catal. Today 258 (2015) 96–102.
[31] M. Ge, C. Cao, S. Li, S. Zhang, S. Deng, J. Huang, Q. Li, K.-Q. Zhang, S.S. Al-deyab, Y. Lai, Nanoscale 7 (2015) 11552–11560.
[32] M. Solís, M.E. Rincón, J.C. Calva, G. Alvarado, Electrochim. Acta 112 (2013) 159–163.
[33] D.-J. Lin, H.-L. Huang, J.-T. Hsu, T.-M. Shieh, L.-J. Fuh, W.-C. Chen, J. Med. Biol. Eng. 33 (2012) 538–544.
[34] J. Xu, W. Wang, M. Shang, E. Gao, Z. Zhang, J. Ren, J. Mater. Hazard. 196 (2011) 426–430.
[35] C.-Y. Chang, Y.-H. Hsieh, Y.-Y. Chen, Int. J. Photoenergy 2012 (2012).
[36] W.H. Lee, C.W. Lai, S.B.A. Hamid, Materials 8 (2015) 2139–2153.
[37] J. Huang, W. Cheuk, Y. Wu, F.S. Lee, W. Ho, J. Nanotechnol. 2012 (2012).
[38] T.S. Natarajan, K. Natarajan, H.C. Bajaj, R.J. Tayade, J. Nanopart. Res. 15 (2013) 1–18.
[39] H. Li, D. Wang, P. Wang, H. Fan, T. Xie, Chem. -Eur. J. 15 (2009) 12521–12527.
[40] T. Marino, R. Molinari, H. García, Catal. Today 206 (2013) 40–45.
[41] K.-C. Chen, Y.-H. Wang, Y.-C. Lu, Catal. Today 175 (2011) 276–282.
[42] E. Azevedo, A. Torres, F. Aquino Neto, M. Dezotti, Braz. J. Chem. Eng. 26 (2009) 75–87.
[43] E.B. Azevedo, F.R. de Aquino Neto, M. Dezotti, Appl. Catal. B Environ. 54 (2004) 165–173.
[44] P. Jin, R. Chang, D. Liu, K. Zhao, L. Zhang, Y. Ouyang, J. Environ. Chem. Eng. 2 (2014) 1040–1047.

Please cite this article in press as: I. Ali, et al., Anodization of bismuth doped TiO_2 nanotubes composite for photocatalytic degradation of phenol in visible light, Catal. Today (2016), http://dx.doi.org/10.1016/j.cattod.2016.03.029